Ring-opening polymerization of Amino Acid N-Carboxyanhydrides with Unprotected/Reactive Side Groups. II. L-Hydroxyproline N-Carboxyanhydride

Letian Wang, Xinyi Zhu, Chenming Tang, Xiaodong Jing, Yahui He, and Hua Lu*

Beijing National Laboratory for Molecular Sciences, Center for Soft Matter Science and Engineering, Key Laboratory of Polymer Chemistry and Physics of Ministry of Education, College of Chemistry and Molecular Engineering, Peking University, Beijing 100871, People's Republic of China.

Corresponding Author: chemhualu@pku.edu.cn (H.L.)

Abstract

Poly-L-hydroxyproline (PHyp) is a synthetic analogue of collagen, the most abundant protein for animals, and holds immense potential for broad biomedical applications. The synthesis of PHyp, however, involves inefficient protection-deprotection steps and has been restricted to relatively low molecular weight (MW) and linear topology. Here, we report the ring-opening polymerization (ROP) of unprotected hydroxyproline *N*-carboxyanhydrides (Hyp-NCA) for the facile one-step synthesis of PHyp with tunable linear or branching topologies. Employing an innovative water-assisted ultrafast polymerization technique, the research achieves the synthesis of linear PHyp with MW up to 7.5 kDa, featuring adjustable terminal groups and narrow dispersity. The study further introduces a tertiary amine-triggered one-pot polymerization method in DMSO, which leads to the preparation of branched PHyp (B-PHyp) with MW up to 438 kDa, ~40 times higher than previous record of PHyp. Facile post-polymerization modification of B-PHyp affords injectable hydrogels with a critical gelization concentration as low as 1.0%. The polymers, characterized by their distinctive collagen-like polyproline type II (PPII) helices, offer significant prospects in drug delivery, wound healing, and other biomedical applications.

Introduction

Collagen is the most predominant protein type in animals, constituting approximately 25-30% of the total animal protein content. Its crucial functions include structural support, tissue repair, and physical protection. 4-Hydroxyproline (Hyp), an amino acid abundant in collagen, is synthesized through post-translational modification of proline mediated by 4-prolyl hydroxylase.[1-2] Hyp accounts for approximately 14% of the total amino acid composition in collagen, making it more abundant than several canonical amino acids. Previous research has demonstrated that Hyp plays a vital role in proper formation of collagen fibrils, with its 4-*trans*-hydroxyl group stabilizing the secondary structure known as polyproline type II (PPII) helix[3-4] and further promoting the self-assemble of collagen unimer into the characteristic triple helical structure.[5-6]

Compared with the right-handed α-helix, the PPII helix exhibits a more extended, left-handed conformation resembling a 3_2 helix structure where all amide bonds adopt *trans* conformation.[7-10]Approximately 5% of the overall protein secondary structure is associated with PPII helical conformation, which often serves as a scaffold or recognition motif involved in biological macromolecular interactions within living organisms.[10-12]

Synthetic polypeptides, also known as poly(amino acid)s, are biomimetic polymers with inherent biocompatibility, tunable biodegradability, and well-defined secondary structures akin to peptides and proteins, holding enormous application potential in the field of materials science and biomedicine.[13-17] Polypeptides are usually prepared by the ring-opening polymerization (ROP) of *N*-carboxyanhydride (NCA) with well-controlled number-average molecular weight (M_n), dispersity ($Đ$), end groups, and topological structure.[16, 18-20]Among all the polypeptides, poly-L-proline (PLP) has been an extensively studied model of PPII helix.[21-22] Poly-L-hydroxyproline (PHyp), less explored, represents another important model for comprehending the biology and biomaterials associated with the PPII helix additional to PLP. Along this direction, Hyp-based low molecular weight (MW) oligomers and its derivatives synthesized via solid-phase peptide synthesis (SPPS) have garnered significant progresses across diverse fields such as organocatalysis, drug delivery, and cell membrane penetrating.[23-33] However, it remains a great challenge to produce PHyp with high MW at a large scale using SPPS.[34-35] Previously, *O*-acetylated Hyp NCA monomer (AcHyp-NCA) had been synthesized and polymerized to afford *O*-acetylated PHyp (PAcHyp, Figure 1A).[36] The crystal structure of PHyp was subsequently studied.[37-38] Gkikas and coworkers copolymerized *O*-Benzyl-L-hydroxyproline NCA (BLHyp-NCA) and γ-Benzyl-L-glutamate NCA (BLG-NCA) in THF to prepare di-block copolymers bearing two different helical structures, which self-assembled into interesting zigzag lamellar structure.[39] Recently, Kramer et al. successfully achieved the polymerization of AcHyp-NCA using Ni- and Co-based organometallic catalysts, affording PAcHyp with M_n up to 15.3 kg/mol.[40] The subsequent deprotection of PAcHyp led to the generation of

water-soluble PHyp. More recently, Hyp-drived polypeptides and poly(thio)esters have been prepared with various functionalities and diverse application potentials.[41-44] In spite of these remarkable advances, current methods all require protection of the hydroxyl group and can only offer linear PHyp, the protection-free synthesis of PHyp with ultra-high MW and non-linear topologies remains largely elusive.

Recently, our group developed a robust approach enabling the moisture-tolerant synthesis of various challenging unprotected NCA (UP-NCAs) monomers bearing reactive functional groups such as hydroxy, thiol, and carboxylic acid in the side chain.[45] These compounds include cysteine NCA (Cys-NCA), D-penicillamine NCA (Pen-NCA), serine NCA (Ser-NCA), glutamic NCA (Glu-NCA), and hydroxyproline NCA (Hyp-NCA). By studying the polymerization of these UP-NCAs, it is possible to eliminate the laborious protection-deprotection steps, and more importantly, create unprecedented structures by harnessing the reactivity of the side groups. Previously, the (co-)ROP of Glu-NCA, Cys-NCA, and Pen-NCA have been reported, affording poly-L-glutamic acid, branched cysteine-containing polypeptides, and poly-D-penicillamine with various rich functionalities, respectively.[45-47] In this study, we systematically investigated the ROP behavior of Hyp-NCA bearing a secondary hydroxy group (Figure 1B). Our results revealed that Hyp-NCA can be one-pot polymerized in either mixed acetonitrile/water (ACN/H_2O) to afford linear PHyp with M_n up to 7.5 kg/mol and narrow $Đ$ below 1.30, or anhydrous DMSO to produce branched PHyp (B-PHyp) with ultra-high weight-average molecular weight (M_w) up to 438 kg/mol. The acylation of B-PHyp with various anhydrides provides a convenient approach to further tune and enrich the property of B-PHyp, including the generation of physical hydrogels with the critical gelation concentration (CGC) as low as (1%).

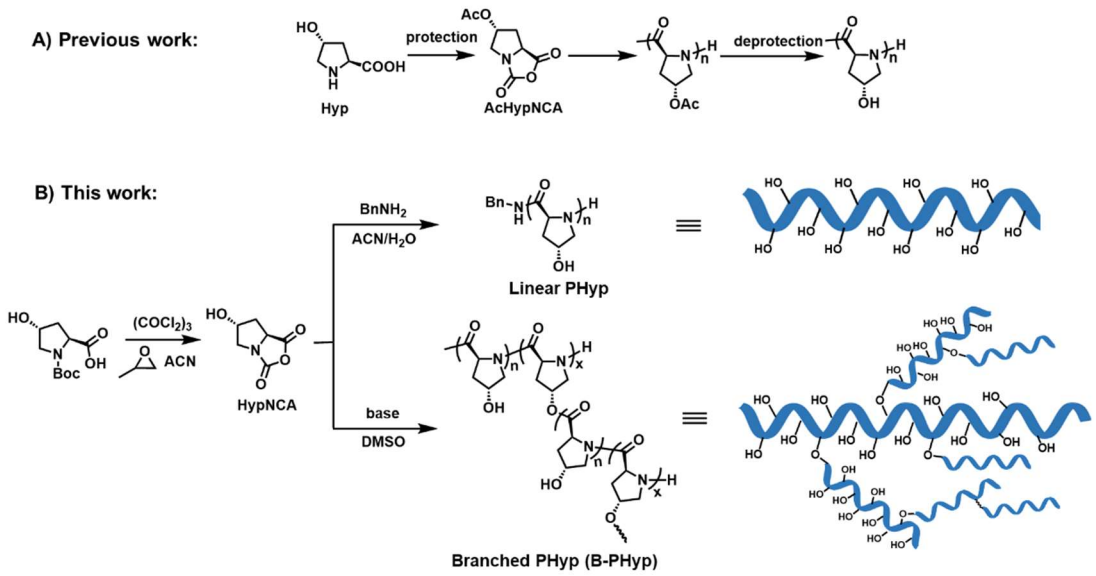

Figure 1: A) Typical synthesis of linear PHyp via the ROP of AcHyp-NCA followed by deprotection; B) This work: synthesis of linear and branched PHyp through the ROP of Hyp-NCA in mixed ACN/H_2O or anhydrous DMSO, respectively.

Results and Discussion

Our research group has recently developed an ultra-fast and controllable ROP method for proline NCA (Pro-NCA) via an unprecedented water-assisted approach, affording PLP with high yield, well-defined end groups, predictable M_n, and narrow $Đ$ within 1-5 minutes.[48] This simple method has been successfully adapted by independent groups generating PLP with fascinating thermal responsiveness and ice inhibition properties.[49-50] Based on the structural similarity between Hyp and proline, we hypothesized that Hyp-NCA (Fig. S1) may exhibit similar ultra-fast polymerization behavior as Pro-NCA does when assisted by water.

To investigate this hypothesis, we studied the benzyl amine-mediated ROP of Hyp-NCA in mixed ACN/H_2O (v/v = 1/1) by following the previously optimized condition for the ROP of Pro-NCA.[48] As expected, the observed phenomenon during the Hyp-NCA polymerization process was similar to that observed for Pro-NCA: immediately after the addition of initiator to monomer, there was a rapid release of CO_2 followed by the completion of monomer within five minutes. Unlike the ROP of Pro-NCA that maintained a homogeneous system throughout the polymerization process, however, the ROP of Hyp-NCA resulted in a phase-separated system that were redissolvable by

adding more water after the monomer consumption. This difference was attributed to the higher hydrophilicity of PHyp over PLP. Size exclusion chromatography (SEC) revealed unimodal and sharp peaks ($Đ$ = 1.12 – 1.14) for the reaction mixtures at the feeding monomer-to-initiator ($[M]_0/[I]_0$) ratios of 25/1, 50/1 (Figure 2A). The obtained M_n (M_n^{obt}) of PHyp, determined by SEC equipped with multi-angle light scattering (MALS), were 2.8, and 5.4 kg/mol (entry 1-2, Table 1), respectively, all within ± 10% deviation compared with the calculated M_n (M_n^{cal}). MALDI-TOF mass spectrometry of a 25-mer of PHyp (entry 1, Table 1) gave a set of peaks that were assignable to PHyp with $C_6H_5CH_2NH$- and H- as the α and ω ends, respectively (Figure 2B). Overall, the MALDI-TOF results echoed the SEC results in M_n^{obt}, indicating controlled polymerization under the designated conditions with minimal hydrolysis or water-initiated polymerization. At a feeding ratio of 100/1, however, the M_n^{obt} of PHyp was only 7.5 kg/mol, significantly lower that the M_n^{cal} value of 11.4 kg/mol (Table 1, entry 3). While the ROP of Pro-NCA at the feeding ratio of 100/1 still maintained its M_n control under similar conditions, the deteriorated M_n control of Hyp-NCA ROP was likely, again, due to the enhanced hydrophilicity and thus faster hydrolysis of monomer. PHyp exhibited excellent water solubility with a stable PPII helix even at elevated temperatures up to 85 °C according to circular dichroism (CD) spectra (Figure 2C), in distinct contrast with PLP that showed thermosensitivity and PPII helix-to-PPI helix transition.[50] Hyp-NCA and Pro-NCA were also successfully copolymerized at a total monomer-to-initiator ratios of 50/1 in mixed ACN/H_2O, affording copolymers with $Đ$ below 1.12, predictable Hyp-to-Pro ratios (Fig. S2), and M_n^{obt} close to M_n^{cal} (entry 4-7, Table 1). Furthermore, we also attempted to initiate the ROP of Hyp-NCA in mixed ACN/phosphate buffer (PBS, pH = 7.4) using a model protein, enhanced green fluorescent protein (EGFP) (Figure 2D). Sodium dodecyl sulfate polyacrylamide gel electrophoresis (SDS-PAGE) showed a smeared new band at upper MW region and the disappearance of EGFP (Figure 2E). SEC revealed a narrow, symmetric, single peak with a complete shift in retention time compared with the native EGFP (Figure 2F), corroborating the successful generation of the desired EGFP-PHyp conjugate via the

so-called “grafting-from” approach. EGFP and EGFP-PHyp were found to display comparable fluorescence intensity, suggesting good preservation of the protein function (Figure 2F).

Table 1：Benzylamine-Initiated Ring-Opening Polymerization of Hyp-NCA or Hyp-NCA/Pro-NCA in ACN/H_2O

Entry	Name	NCA	[NCA]/[I]	M_n^{cal} (kg/mol) [a]	M_n^{obt} (kg/mol) [b]	Hyp/Pro[c]	$Đ$ [b]
1	$PHyp_{25}$	Hyp	25/1	2.9	2.8	-	1.12
2	$PHyp_{50}$	Hyp	50/1	5.8	5.4	-	1.14
3	$PHyp_{100}$	Hyp	100/1	11.4	7.5	-	1.30
4	Hyp_{40}-Pro_{10}	Hyp/Pro	40/10/1	5.6	4.7	3.9/1.1	1.12
5	Hyp_{30}-Pro_{20}	Hyp/Pro	30/20/1	5.4	4.2	3.1/1.9	1.10
6	Hyp_{20}-Pro_{30}	Hyp/Pro	20/30/1	5.3	5.2	1.9/3.1	1.07
7	Hyp_{10}-Pro_{40}	Hyp/Pro	10/40/1	5.1	4.6	0.9/4.1	1.11

[a]Calculated from feeding [NCA]/[I]. [b]Obtained from aqueous SEC equipped with a multi-angle light scattering and a reflective index detectors in 1 × PBS (pH = 7.4) mobile phase; *dn/dc* (658 nm) values were measured as 0.159 for PHyp. [c]Calculated from ^{1}H-NMR spectroscopy (Figure S2).

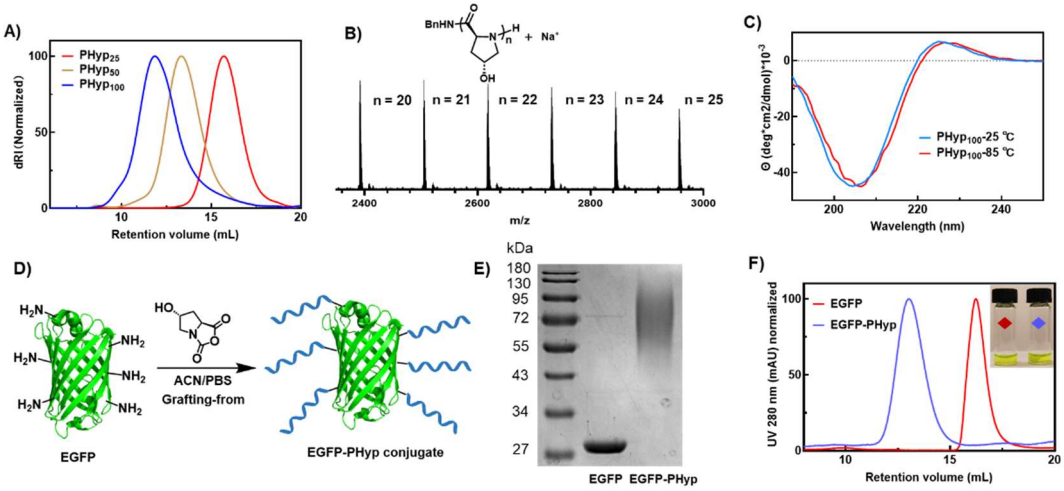

Figure 2. Characterization of PHyp and EGFP-PHyp conjugate. A) SEC chromatogram of PHyp (Table 1, entries 1−3); B) MALDI-TOF mass spectrometry of $PHyp_{25}$; C) CD spectra of $PHyp_{100}$ at 25 ℃ (blue) and 85 ℃ (red) exhibiting typical left-handed PPII helices; D) Cartoon illustration of the EGFP-initiated ROP of Hyp-NCA; E) SDS-PAGE characterization of EGFP and the EGFP-PHyp conjugate; F) aqueous SEC characterization of EGFP-PHyp prepared by EGFP-mediated ROP of Hyp-NCA; inset: snapshots of EGFP and the EGFP-PHyp conjugate.

Different from PLP that was hardly soluble in common organic solvents,

interestingly, both Hyp-NCA and PHyp were highly soluble in DMSO. Given this fact, we next investigated the ROP of Hyp-NCA in DMSO using organic bases. We postulated that the hydroxyl group of Hyp-NCA could be activated by organic bases to exhibit nucleophilicity properties, making a small portion of Hyp-NCA acting as inimer, i.e. a compound with the dual role of initiator and monomer, and producing (hyper)branched polymers.[51-60] Consequently, we speculated that the ROP of Hyp-NCA in DMSO could afford B-PHyp with ester bond, secondary amine, and peptide bonds as the dendritic (D), terminal (T), and linear (L) units, respectively (Figure 1B). [61-65] To explore this hypothesis, we employed common organic bases such as DIPEA (conjugate acid pK_a ~ 10) and DBU (conjugate acid pK_a = 13.9)[66] as the catalyst (Table 2). At an initial monomer concentration $[Hyp\text{-}NCA]_0$ of 2.0 M and fixed [Hyp-NCA]/[DIPEA] ratio of 50/1, after a short induction period, the reaction system rapidly generated gas and becomes viscous gradually. Aqueous SEC analysis using Superdex 75 indicated that the MW of the obtained polymer B-PHyp-1 exceeded the upper limit of the column (70 kDa for protein). Treating B-PHyp-1 with a 0.5 M NaOH solution for 3 hours resulted in a complete shift of the SEC trace towards the lower molecular weight region (Figure 3A), suggesting a significant reduction in MW due to the hydrolysis of the branching ester units. FT-IR characterization of B-PHyp-1 revealed characteristic absorption peaks at 1735 cm^{-1} and 1653 cm^{-1} (Figure 3B), which were attributed to ester and amide carbonyl stretches, respectively (assignment based on PAcHyp obtained by ROP of AcHyp-NCA in ACN/H_2O, Figure S3). Moreover, proton nuclear magnetic resonance spectroscopy (^{1}H-NMR) depicted a small peak at ~ 5.36 ppm for the designated B-PHyp-1, which was absent in the linear PHyp obtained in ACN/water system and assignable to the γ-H on the pyrrolidone ring of Hyp after acylation (Figure 3C). Overall, the above experimental evidence fully supported the branched topology hypothesis. To obtain more accurate MW of B-PHyp-1, the previous Superdex 75 SEC column was replaced with a Superose 6 Increase column, which gave a M_n^{obt} of 32.3 kg/mol, M_w^{obt} of 71.4 kg/mol, and $Đ$ of 2.55 (Figure 3D and entry 1, Table 2). Given the high MW and dispersity of the product, M_w^{obt} are used in further descriptions of B-PHyp for its ability to better reflect the properties of these polymers.

To calculate the degree of branching (DB) of B-PHyp-1, we employed the formula DB = $(D + T)/(D + T + L)$, where D, T, and L represent the number of dendritic, terminal, and linear units, respectively[67]. According to the proposed structure of B-PHyp (Figure 1B), the sum of $D + T + L$ roughly equals to the degree of polymerization (DP), and D is always one unit smaller than T ($D = T - 1$). Therefore, the formula can be simplified to DB = $2T$/DP when the M_w of B-PHyp was reasonably high. Of note, the value of T/DP (secondary amine content) was obtainable with UV-Vis spectrometry measuring the characteristic absorbance of the reaction product of *p*-toluene diazonium salt with secondary amines, a method developed by Raj et al.[68] Thus, the DB of B-PHyp-1 was calculated as ~0.24 (Table 2, see SI, Figure S4,Table S1 for detailed method).

Next, we varied the [Hyp-NCA]/[DIPEA] ratio in the range from 100/1 to 2000/1 to regulate the molecular weight and DB of the resulting B-PHyp (entry 2-6, Table 2). Increasing the $[M]_0/[DIPEA]_0$ ratio led to substantially higher M_w, which exceeded the upper separation limit of the Superose 6 Increase column when the ratio was beyond 500/1 (Figure S5). The SEC traces of B-PHyp-4, -5 and -6 (entry 4-6, Table 2) was obtained after the separation column was replaced to MIXED-H columns (Figure 3E). DIPEA-2000 reached an absolute M_w value of 438 kg/mol, which was approximately 40 times higher than previously reported maximum molecular weights for PHyp.[40] The DB of B-PHyp, however, became substantially smaller at higher [Hyp-NCA]/[DIPEA] ratios (Table 2). When a stronger organobase DBU was used to mediate the ROP, similar to the case of DIPEA, higher $[M]_0/[DBU]_0$ ratios gave greater M_w and smaller DB of B-PHyp (entry 7-9, Table 2 and Figure 3D). Of note, SEC revealed a M_w of B-PHyp-8 of 55.4 kg/mol (entry 8, Table 2), smaller than the M_w of B-PHyp-1 at the same $[M]_0/[base]_0$ ratio mediated by DIPEA (entry 1, Table 2). However, the DB of B-PHyp-8 was calculated as 0.38, greater than that of B-PHyp-1 (entry 8 and 1, Table 2). Thus, the higher basicity appeared to give smaller M_n but greater DB. Circular dichroism spectroscopy revealed that B-PHyp still exhibited a characteristic PPII helix pattern, although with decreased helicity compared to linear PHyp (Figure 3F). Moreover, the greater the DB, the lower the helicity was observed. Similar to the linear PHyp, B-PHyp also displayed unchanged PPII helicity at an elevated temperature up to 85 °C according

to CD analysis (Figure S6).

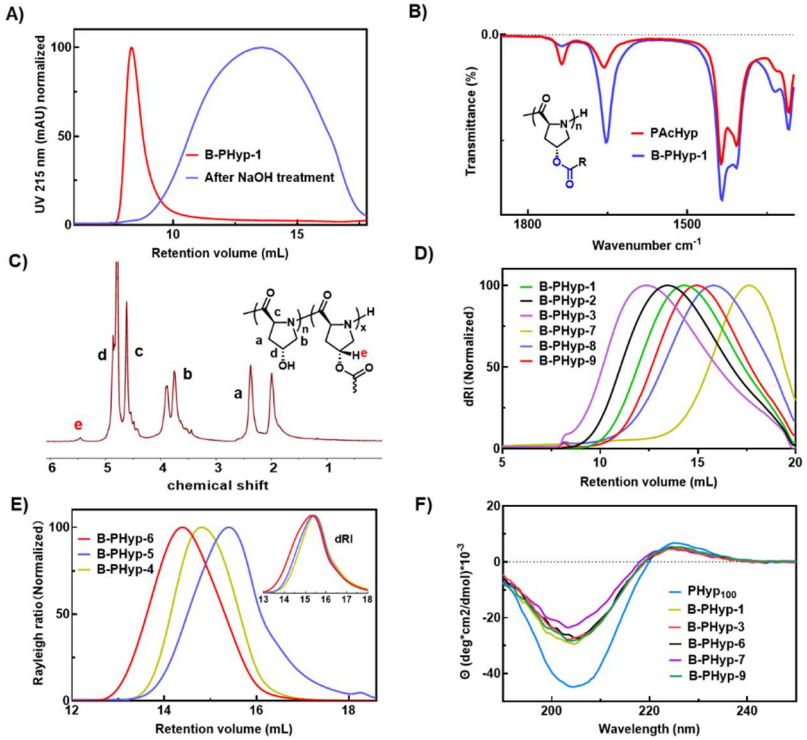

Figure 3. Characterizations of B-PHyp: A) SEC chromatogram of B-PHyp-1, before (red) and after (blue) NaOH treatment; note the red curve was eluted at the dead volume (8 mL) of the Superdex 75 column. B) Overlay of FT-IR Spectra of PAcHyp and B-PHyp-1. C) ^{1}H-NMR spectrum of B-PHyp-1 in D_2O. D) SEC chromatogram of B-PHyp (Table 2, entries 1-3, 7-9) using Superose 6 Increase columns from Cytiva. E) MALLS-SEC chromatogram of B-PHyp (Table 2, entries 4-6) using PL Aquagel-OH MIXED-H columns from Agilent. Inset: RI signals. F) CD spectra of B-PHyp (Table 2, entries 1, 3, 6, 7, 9) and $PHyp_{100}$ (Table 1, entry 3) showing typical left-handed PPII helices.

Table 2：ROP of Hyp-NCA mediated by DIPEA or DBU in DMSO

Entry	Name	Base	[NCA]/ [Base]	M_n (kg/mol) [a]	M_w (kg/mol) [a]	$Đ$ [a]	Amino content [b]	Degree of branching [c]
1	B-PHyp-1	DIPEA	50	32.3	71.4	2.55	12%	0.24
2	B-PHyp-2	DIPEA	100	36.7	110	3.01	11%	0.22
3	B-PHyp-3	DIPEA	200	65.2	148	2.27	7%	0.14
4	B-PHyp-4	DIPEA	500	66.9	244	3.65	1%	0.02
5	B-PHyp-5	DIPEA	1000	87.4	291	3.32	1%	0.02
6	B-PHyp-6	DIPEA	2000	135	438	3.24	1%	0.02
7	B-PHyp-7	DBU	25	12.9	25.5	1.98	28%	0.56
8	B-PHyp-8	DBU	50	16.6	55.4	3.35	19%	0.38
9	B-PHyp-9	DBU	100	34.0	76.6	2.26	12%	0.24

[a] Obtained from aqueous SEC equipped with multi-angle light scattering and reflective index detectors in 1 × PBS (pH = 7.4) mobile phase; *dn/dc* (658 nm) values were measured as 0.159 for B-PHyp. [b] Calculate using the reaction of *p*-toluene diazonium salt with secondary amines.

[c] DB = 2*T*/DP.

Next, with the in-situ FT-IR spectroscopy, we examined the kinetic feature of different bases-mediated ROP of Hyp-NCA in DMSO (Figure 4). At a [Hyp-NCA]/[B] ratio of 100/1, benzyl amine was found sluggish in mediating the ROP, with a less than 20% monomer conversion after 2-hour incubation. In contrast, when DIPEA was used at the same [Hyp-NCA]/[B] ratio, CO_2 bubbles were rapidly generated after a 14.5 min induction period and the system became viscous soon, reaching complete monomer conversion within 50 minutes (Figure 4A). DBU gave a similar kinetic feature to DIPEA, i.e. a 12.5 min short induction period followed by a self-accelerating, explosive consumption stage of monomer within 25 min (Figure 4A). Compared to the DIPEA-mediated ROP, the induction period was shorter and ROP was faster when DBU was used as the base. Both reactions did not follow a simple first-order kinetics, suggesting complicated reaction process. This self-accelerating effect became more pronounced with increasing base equivalents or reaction concentration (Figure 4B).

To obtain the relationship of monomer conversion with the M_w and DB, we quenched the ROP in DMSO by excessive mesylate at various time points, followed by precipitation of the solution in acetone to remove unreacted Hyp-NCA monomer and potential small molecular species from the crude product. Subsequently, the precipitates were dissolved in water, purified using a flash SEC column (PD-10), and then lyophilized to obtain pure polymers. The M_n, M_w and $Đ$ of the polymer intermediates at the designated monomer conversions (Figure S7) were determined via SEC analysis (Figure 4C). The *DB* was again quantified using Raj's method to calculate the ratio of secondary amines to amides (Figure S8 and Table S2). It was found that M_w increased and *DB* decrease steadily as monomer was consumed (Figure 4D). Notable, M_w increased slowly at the early stage of the ROP and more rapidly at the late stage, somewhat resembling the classical step-growth polymerization pattern. The dispersity of the B-PHyp was expanded from 2.40 to 4.35 as the reaction preceded (Figure S9).

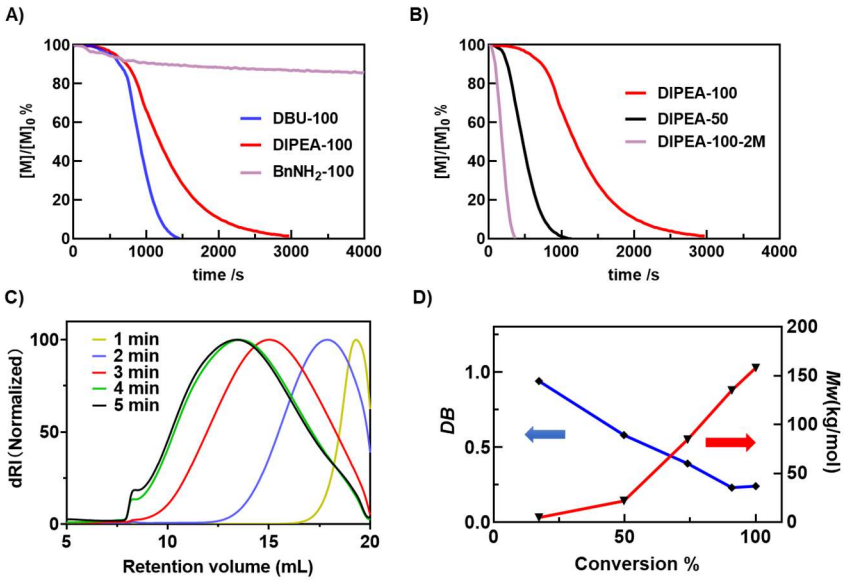

Figure 4: Kinetic study of ROP of Hyp-NCA in DMSO. A) plots of monomer consumption ($[M]/[M]_0$) versus time; the reactions were mediated by different bases; $[M]_0/[I]_0$ ratio of 100/1, $[M]_0$ = 1.0 M; B) plots of monomer consumption ($[M]/[M]_0$) versus time; the reactions were mediated with DIPEA at varied $[M]_0/[B]_0$ ratios, $[M]_0$ = 1.0 or 2.0 M ; C) SEC chromatogram of polymerization system of B-PHyp-2 at varied quenching time ; D) Plots of M_w and *DB* of B-PHyp-2 as a function of monomer conversion.

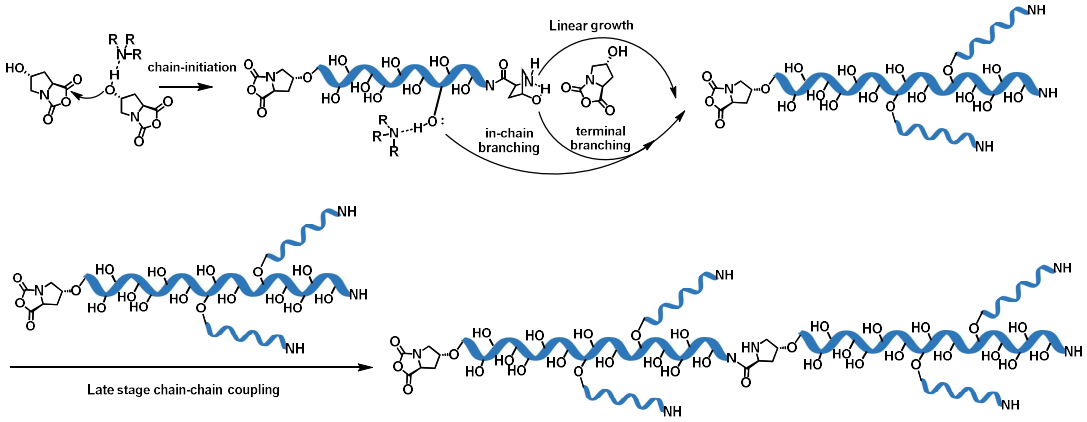

Figure 5: Proposed mechanism of the ROP of Hyp-NCA in DMSO.

Based on these kinetic results, we proposed a plausible mechanism for the tertiary amine-mediated ROP of Hyp-NCA in DMSO. Tertiary amines first activated hydroxy group of Hyp-NCA, which initiated the ROP by nucleophilic attack a new Hyp-NCA monomer, generating a secondary amine for further linear chain propagation (Figure 5). As the basicity of DIPEA and DBU were insufficient for complete deprotonation of hydroxyl groups, an induction period occurred initially with the length of the induction

period reversely depended on the basicity (Fig. 4A-B). During the chain growth stage, the hydroxyl group competed with secondary amines to react with Hyp-NCA, generating more secondary amine terminals and the ester bond-branched topology (Figure 5). As the concentration of secondary amines increased, the reaction underwent self-acceleration in the mid stage (Fig. 4A-B). Of note, the ester-bond (branching) formation can be theoretically divided into two patterns: terminal branching catalyzed by intramolecular secondary amine at the chain end or in-chain branching mediated by tertiary amine (Figure 5). While it is still difficult to evaluate which route was more preferred, the portion of intermolecular activation would gradually increase with the greater basicity or higher concentration of tertiary amine. As hydroxyl group-mediated ring-opening was dominated at the initial stage of the reaction, the polymers featured in slow chain growth, and a great portion of ester linkage and thus higher *DB* (Figure 4D). At the mid- and late stages, the *DB* decreased significantly as the newly generated secondary amines were more efficient in ROP and producing predominantly linear units (Figure 4D). The accelerated increase in M_w after the mid-stage (i.e. ~50% monomer conversion in Figure 4D) suggested, as the remaining monomer concentration decreases, the probability of chain-chain coupling between secondary amines and the overhanging NCA rings at the chain terminal grew substantially (Figure 5).

Next, we attempted to tune the property of B-PHyp by acylation of the branched polymers with rich functionalities (Figure 6A). In the DMSO polymerization system with [Hyp-NCA]/[DIPEA] of 1000/1, various anhydride/activated ester and triethylamine were added in situ after the polymerization. When 0.5 equivalent acetic anhydride (relative to $[M]_0$) was added, ^{1}H-NMR spectroscopy showed that the degree of acetylation reached ~40% (Figure S10), and the resulting product B-PHyp-Ac formed a physical hydrogel with a storage modulus (G') of ~300 Pa at a solid content as low as 1% (Figure 6B). The resultant hydrogel displayed typical shear-thinning behavior, enabling injection through a syringe, while exhibiting reversible gel-liquid phase transition (Figure 6C, D). With further increased degree of acetylation, the mechanical strength of the resulting gel was enhanced accordingly (Figure S11). Apart from acetylation, modification with succinic anhydride (SA) and lipoic acid activated

ester (LA) was also proven successful (Figure 6E, S12, and S13). 5% lipoyl modification of B-PHyp also yielded a physical hydrogel at a 2% solid content (Figure S13). B-PHyp modified with succinic anhydride (B-PHyp-SA) excellent cell adhesion ability comparable to Sodium hyaluronate (HA), an important component of extracellular cell matrix (Figure 6F).

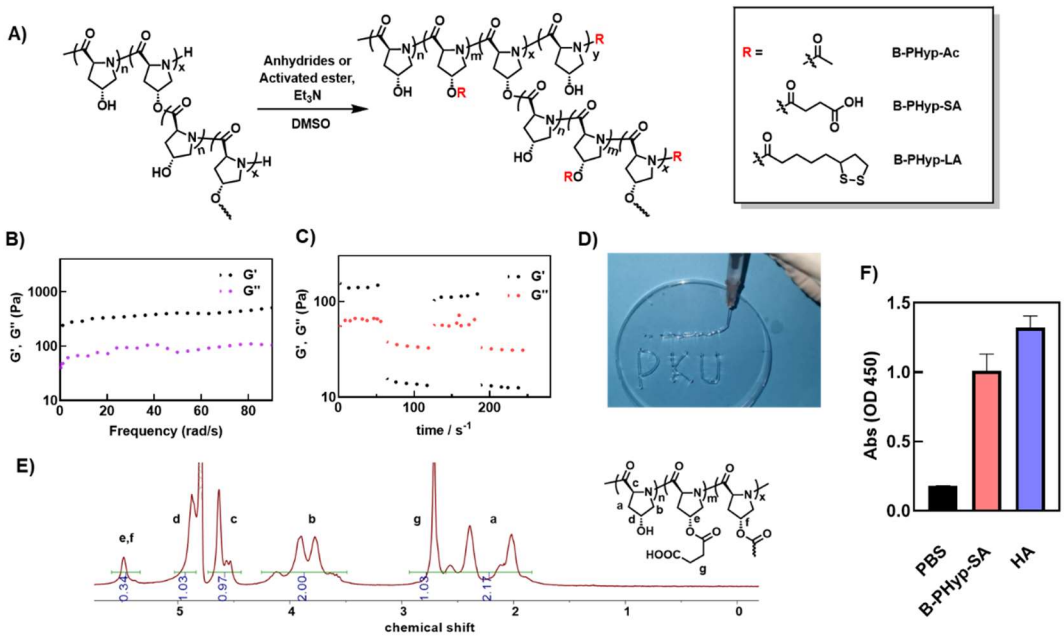

Figure 6: Acylation of B-PHyp. A) scheme of the acylation; B) oscillation frequency scanning curve and C) gradient amplitude scanning curve of the B-PHyp-Ac hydrogel (acetylation degree 40%, solid content 2%); D) a photograph demonstrating the injectability of the hydrogel; E) ^{1}H-NMR spectrum of B-PHyp-SA in D_2O (acylation degree 30%); F) BALB/3T3 Cell adhesion results of B-PHyp-SA and hyaluronic acid (HA, the positive control).

Conclusion

To summarize, the polymerization behaviors of Hyp-NCA was thoroughly investigated in this study. A water-assisted ultrafast polymerization of Hyp-NCA yielded linear PHyp with tunable terminal groups and M_n up to 7.5 kDa. The method also allowed the facile generation of protein-PHyp conjugates via the grafting from approach in aqueous phase. Additionally, we designed and implemented a one-pot polymerization reaction of Hyp-NCA in DMSO to obtain B-PHyp by taking advantage of the unprotected hydroxy group. This versatile polymerization reaction allowed for tunable degrees of branching and yields ultra-high M_w polymers up to 438 kDa.

Furthermore, facile acetylation enabled the post-modification of these polymers into physical hydrogels at low solid contents. These linear or branched PHyp all bearing unique and collagen-like PPII helices, holding great potential for applications in polymeric therapeutics, drug delivery systems, wound healing dressings, biological adhesives, and many other related fields.

Author Information

Corresponding Author

Hua Lu − *Beijing National Laboratory for Molecular Sciences, Center for Soft Matter Science and Engineering, Key Laboratory of Polymer Chemistry and Physics of Ministry of Education, College of Chemistry and Molecular Engineering, Peking University, Beijing 100871, People's Republic of China;* orcid.org/0000-0003-2180-3091; Email: chemhualu@pku.edu.cn

Authors

Letian Wang − *Beijing National Laboratory for Molecular Sciences, Center for Soft Matter Science and Engineering, Key Laboratory of Polymer Chemistry and Physics of Ministry of Education, College of Chemistry and Molecular Engineering, Peking University, Beijing 100871, People's Republic of China*

Xinyi Zhu − *Beijing National Laboratory for Molecular Sciences, Center for Soft Matter Science and Engineering, Key Laboratory of Polymer Chemistry and Physics of Ministry of Education, College of Chemistry and Molecular Engineering, Peking University, Beijing 100871, People's Republic of China*

Chenming Tang − *Beijing National Laboratory for Molecular Sciences, Center for Soft Matter Science and Engineering, Key Laboratory of Polymer Chemistry and Physics of Ministry of Education, College of Chemistry and Molecular Engineering, Peking University, Beijing 100871, People's Republic of China*

Xiaodong Jing − *Beijing National Laboratory for Molecular Sciences, Center for Soft Matter Science and Engineering, Key Laboratory of Polymer Chemistry and Physics of Ministry of Education, College of Chemistry and Molecular Engineering, Peking University, Beijing 100871, People's Republic of China*

Yahui He − *Beijing National Laboratory for Molecular Sciences, Center for Soft Matter Science and Engineering, Key Laboratory of Polymer Chemistry and Physics of Ministry of Education, College of Chemistry and Molecular Engineering, Peking University, Beijing 100871, People's Republic of China*

Acknowledgments

This work is supported by National Natural Science Foundation of China (22331002 and 22125101), Beijing Natural Science Foundation Key Project (Z220023), Peking University Clinical Medicine plus X (ZX002), and the Open Funding Project of the State Key Laboratory of Biochemical Engineering & Key Laboratory of Biopharmaceutical Preparation and Delivery (No. 2023KF-01). The authors want to thank Dr. Bowen Qi for helping the cell adhesion assay and Tsinghua University Branch of China National Center for Protein Sciences (Beijing) for the MALLS-SEC instruments.

References

1. Holster, T.; Pakkanen, O.; Soininen, R.; Sormunen, R.; Nokelainen, M.; Kivirikko, K. I.; Myllyharju, J., Loss of assembly of the main basement membrane collagen, type IV, but not fibril-forming collagens and embryonic death in collagen prolyl 4-hydroxylase I null mice. *J. Biol. Chem.* **2007,** *282* (4), 2512-2519.

2. Friedman, L.; Higgin, J. J.; Moulder, G.; Barstead, R.; Raines, R. T.; Kimble, J., Prolyl 4-hydroxylase is required for viability and morphogenesis in Caenorhabditis elegans. *Proc. Natl. Acad. Sci. U.S.A.* **2000,** *97* (9), 4736-4741.

3. Best, R. B.; Merchant, K. A.; Gopich, I. V.; Schuler, B.; Bax, A.; Eaton, W. A., Effect of flexibility and cis residues in single-molecule FRET studies of polyproline. *Proc. Natl. Acad. Sci. U.S.A.* **2007,** *104* (48), 18964-18969.

4. Wilhelm, P.; Lewandowski, B.; Trapp, N.; Wennemers, H., A Crystal Structure of an Oligoproline PPII-Helix, at Last. *J. Am. Chem. Soc.* **2014,** *136* (45), 15829-15832.

5. Shoulders, M. D.; Raines, R. T., Collagen structure and stability. *Annu. Rev. Biochem.* **2009,** *78*, 929-958.

6. Li, X.; Zhang, Q.; Yu, S. M.; Li, Y., The Chemistry and Biology of Collagen Hybridization. *J. Am. Chem. Soc.* **2023,** *145* (20), 10901-10916.

7. Forsythe, K. H.; Hopfinger, A. J., The Influence of Solvent on the Secondary Structures of Poly(L-

alanine) and Poly(L-proline). *Macromolecules* **1973,** *6* (3), 423-437.
8. Steinberg, I. Z.; Harrington, W. F.; Berger, A.; Sela, M. N.; Katchalski, E., The Configurational Changes of Poly-L-proline in Solution. *J. Am. Chem. Soc.* **1960,** *82*, 5263-5279.
9. Shi, L.; Holliday, A. E.; Shi, H.; Zhu, F.; Ewing, M. A.; Russell, D. H.; Clemmer, D. E., Characterizing intermediates along the transition from polyproline I to polyproline II using ion mobility spectrometry-mass spectrometry. *J. Am. Chem. Soc.* **2014,** *136* (36), 12702-12711.
10. Narwani, T. J.; Santuz, H.; Shinada, N.; Melarkode Vattekatte, A.; Ghouzam, Y.; Srinivasan, N.; Gelly, J. C.; de Brevern, A. G., Recent advances on polyproline II. *Amino Acids* **2017,** *49* (4), 705-713.
11. Rath, A.; Davidson, A. R.; Deber, C. M., The structure of "unstructured" regions in peptides and proteins: role of the polyproline II helix in protein folding and recognition. *Biopolymers* **2005,** *80* (2-3), 179-185.
12. Meirson, T.; Bomze, D.; Kahlon, L.; Gil-Henn, H.; Samson, A. O., A helical lock and key model of polyproline II conformation with SH3. *Bioinformatics* **2020,** *36* (1), 154-159.
13. Deming, T. J., Synthesis of Side-Chain Modified Polypeptides. *Chem. Rev.* **2015,** *116* (3), 786-808.
14. Song, Z.; Han, Z.; Lv, S.; Chen, C.; Chen, L.; Yin, L.; Cheng, J., Synthetic polypeptides: from polymer design to supramolecular assembly and biomedical application. *Chem. Soc. Rev.* **2017,** *46* (21), 6570-6599.
15. Shen, W.; He, P.; Xiao, C.; Chen, X., From Antimicrobial Peptides to Antimicrobial Poly(alpha-amino acid)s. *Adv. Healthc. Mater.* **2018,** *7* (20), e1800354.
16. Rasines Mazo, A.; Allison-Logan, S.; Karimi, F.; Chan, N. J.; Qiu, W.; Duan, W.; O'Brien-Simpson, N. M.; Qiao, G. G., Ring opening polymerization of alpha-amino acids: advances in synthesis, architecture and applications of polypeptides and their hybrids. *Chem. Soc. Rev.* **2020,** *49* (14), 4737-4834.
17. Zhou, X.; Li, Z., Advances and Biomedical Applications of Polypeptide Hydrogels Derived from alpha-Amino Acid N-Carboxyanhydride (NCA) Polymerizations. *Adv. Healthc. Mater.* **2018,** *7* (15), e1800020.
18. Lu, H.; Wang, J.; Song, Z.; Yin, L.; Zhang, Y.; Tang, H.; Tu, C.; Lin, Y.; Cheng, J., Recent advances in amino acid N-carboxyanhydrides and synthetic polypeptides: chemistry, self-assembly and biological applications. *Chem. Commun.* **2014,** *50* (2), 139-155.
19. Kricheldorf, H. R., Polypeptides and 100 years of chemistry of alpha-amino acid N-carboxyanhydrides. *Angew. Chem. Int. Ed.* **2006,** *45* (35), 5752-5784.
20. Hadjichristidis, N.; Iatrou, H.; Pitsikalis, M.; Sakellariou, G., Synthesis of well-defined polypeptide-based materials via the ring-opening polymerization of alpha-amino acid N-carboxyanhydrides. *Chem. Rev.* **2009,** *109* (11), 5528-5578.
21. Gkikas, M.; Avery, R. K.; Olsen, B. D., Thermoresponsive and Mechanical Properties of Poly(l-proline) Gels. *Biomacromolecules* **2016,** *17* (2), 399-406.
22. Gkikas, M.; Iatrou, H.; Thomaidis, N. S.; Alexandridis, P.; Hadjichristidis, N., Well-Defined Homopolypeptides, Copolypeptides, and Hybrids of Poly(l-proline). *Biomacromolecules* **2011,** *12* (6), 2396-2406.
23. Li, M.; Puschmann, R.; Herdlitschka, A.; Fiedler, D.; Wennemers, H., Delivery of myo-Inositol Hexakisphosphate to the Cell Nucleus with a Proline-Based Cell-Penetrating Peptide. *Angew. Chem. Int. Ed.* **2020,** *59* (36), 15586-15589.
24. Nagel, Y. A.; Raschle, P. S.; Wennemers, H., Effect of Preorganized Charge-Display on the Cell-Penetrating Properties of Cationic Peptides. *Angew. Chem. Int. Ed.* **2017,** *56* (1), 122-126.

25. Dietsche, T. A.; Eldesouky, H. E.; Zeiders, S. M.; Seleem, M. N.; Chmielewski, J., Targeting Intracellular Pathogenic Bacteria Through N-Terminal Modification of Cationic Amphiphilic Polyproline Helices. *J. Org. Chem.* **2020,** *85* (11), 7468-7475.
26. Brezden, A.; Mohamed, M. F.; Nepal, M.; Harwood, J. S.; Kuriakose, J.; Seleem, M. N.; Chmielewski, J., Dual Targeting of Intracellular Pathogenic Bacteria with a Cleavable Conjugate of Kanamycin and an Antibacterial Cell-Penetrating Peptide. *J. Am. Chem. Soc.* **2016,** *138* (34), 10945-9.
27. Kroll, C.; Mansi, R.; Braun, F.; Dobitz, S.; Maecke, H. R.; Wennemers, H., Hybrid bombesin analogues: combining an agonist and an antagonist in defined distances for optimized tumor targeting. *J. Am. Chem. Soc.* **2013,** *135* (45), 16793-16796.
28. Dobitz, S.; Wilhelm, P.; Romantini, N.; De Foresta, M.; Walther, C.; Ritler, A.; Schibli, R.; Berger, P.; Deupi, X.; Behe, M.; Wennemers, H., Distance-Dependent Cellular Uptake of Oligoproline-Based Homobivalent Ligands Targeting GPCRs-An Experimental and Computational Analysis. *Bioconjug. Chem.* **2020,** *31* (10), 2431-2438.
29. Huang, K. Y.; Yu, C. C.; Horng, J. C., Conjugating Catalytic Polyproline Fragments with a Self-Assembling Peptide Produces Efficient Artificial Hydrolases. *Biomacromolecules* **2020,** *21* (3), 1195-1201.
30. Hung, P. Y.; Chen, Y. H.; Huang, K. Y.; Yu, C. C.; Horng, J. C., Design of Polyproline-Based Catalysts for Ester Hydrolysis. *ACS Omega* **2017,** *2* (9), 5574-5581.
31. Yu, L. T.; Hancu, M. C.; Kreutzberger, M. A. B.; Henrickson, A.; Demeler, B.; Egelman, E. H.; Hartgerink, J. D., Hollow Octadecameric Self-Assembly of Collagen-like Peptides. *J. Am. Chem. Soc.* **2023,** *145* (9), 5285-5296.
32. Pandey, A. K.; Naduthambi, D.; Thomas, K. M.; Zondlo, N. J., Proline Editing: A General and Practical Approach to the Synthesis of Functionally and Structurally Diverse Peptides. Analysis of Steric versus Stereoelectronic Effects of 4-Substituted Prolines on Conformation within Peptides. *J. Am. Chem. Soc.* **2013,** *135* (11), 4333-4363.
33. Tian, Z.-Y.; Wang, S.; Lu, H., Hydroxyproline-derived biomimetic and biodegradable polymers. *Curr. Opin. Solid State Mater. Sci.* **2021,** *25* (2), 100902.
34. Townsend, S. D.; Tan, Z.; Dong, S.; Shang, S.; Brailsford, J. A.; Danishefsky, S. J., Advances in proline ligation. *J. Am. Chem. Soc.* **2012,** *134* (8), 3912-3916.
35. Sayers, J.; Karpati, P. M. T.; Mitchell, N. J.; Goldys, A. M.; Kwong, S. M.; Firth, N.; Chan, B.; Payne, R. J., Construction of Challenging Proline-Proline Junctions via Diselenide-Selenoester Ligation Chemistry. *J. Am. Chem. Soc.* **2018,** *140* (41), 13327-13334.
36. Kurtz, J.; Fasman, G. D.; Berger, A.; Katchalski, E., Poly-Hydroxy-L-Proline. *J. Am. Chem. Soc.* **1958,** *80* (2), 393-397.
37. Sasisekharan, V., Structure of poly-L-proline. II. *Acta Crystallogr.* **1959,** *12* (11), 897-903.
38. Cartier, L.; Lotz, B., Frustrated Crystal Structure of Poly(l-hydroxyproline). *Macromolecules* **1998,** *31* (9), 3049-3054.
39. Gkikas, M.; Haataja, J. S.; Seitsonen, J.; Ruokolainen, J.; Ikkala, O.; Iatrou, H.; Houbenov, N., Extended Self-Assembled Long Periodicity and Zig-Zag Domains from Helix–Helix Diblock Copolymer Poly(γ-benzyl-l-glutamate)-block-poly(O-benzyl-l-hydroxyproline). *Biomacromolecules* **2014,** *15* (11), 3923-3930.
40. Detwiler, R. E.; Schlirf, A. E.; Kramer, J. R., Rethinking Transition Metal Catalyzed N-Carboxyanhydride Polymerization: Polymerization of Pro and AcOPro N-Carboxyanhydrides. *J. Am. Chem. Soc.* **2021,** *143* (30), 11482-11489.

41. Bisht, A. S.; Maity, P.; Roy, R. K., Comparison of Thermoresponsive Behavior between Polyproline and Periodically Grafted Polyproline toward Hofmeister Ions: An Explanation of Its Conformational Origin. *Macromolecules* **2023,** *56* (11), 3922-3930.
42. Detwiler, R. E.; McPartlon, T. J.; Coffey, C. S.; Kramer, J. R., Clickable Polyprolines from Azido-proline N-Carboxyanhydride. *ACS Polym. Au* **2023,** *3* (5), 383-393.
43. Yuan, J.; Shi, D.; Zhang, Y.; Lu, J.; Wang, L.; Chen, E.-Q.; Lu, H., 4-Hydroxy-L-Proline as a General Platform for Stereoregular Aliphatic Polyesters: Controlled Ring-Opening Polymerization, Facile Functionalization, and Site-Specific Bioconjugation. *CCS Chem.* **2020,** *2* (5), 236-244.
44. Yuan, J.; Xiong, W.; Zhou, X.; Zhang, Y.; Shi, D.; Li, Z.; Lu, H., 4-Hydroxyproline-Derived Sustainable Polythioesters: Controlled Ring-Opening Polymerization, Complete Recyclability, and Facile Functionalization. *J. Am. Chem. Soc.* **2019,** *141* (12), 4928-4935.
45. Tian, Z. Y.; Zhang, Z. C.; Wang, S.; Lu, H., A moisture-tolerant route to unprotected α/β-amino acid-carboxyanhydrides and facile synthesis of hyperbranched polypeptides. *Nat. Commun.* **2021,** *12* (1), 5810.
46. Yang, M.; Zhang, Z. C.; Yuan, F. Z.; Deng, R. H.; Yan, X.; Mao, F. B.; Chen, Y. R.; Lu, H.; Yu, J. K., An immunomodulatory polypeptide hydrogel for osteochondral defect repair. *Bioact. Mater.* **2023,** *19*, 678-689.
47. Wang, S.; Lu, H., Ring-Opening Polymerization of Amino Acid N-Carboxyanhydrides with Unprotected/Reactive Side Groups. I. d-Penicillamine N-Carboxyanhydride. *ACS Macro Lett.* **2023,** *12* (5), 555-562.
48. Hu, Y.; Tian, Z. Y.; Xiong, W.; Wang, D.; Zhao, R.; Xie, Y.; Song, Y. Q.; Zhu, J.; Lu, H., Water-assisted and protein-initiated fast and controlled ring-opening polymerization of proline N-carboxyanhydride. *Natl. Sci. Rev.* **2022,** *9* (8), nwac033.
49. Judge, N.; Georgiou, P. G.; Bissoyi, A.; Ahmad, A.; Heise, A.; Gibson, M. I., High Molecular Weight Polyproline as a Potential Biosourced Ice Growth Inhibitor: Synthesis, Ice Recrystallization Inhibition, and Specific Ice Face Binding. *Biomacromolecules* **2023,** *24* (6), 2459-2468.
50. Badreldin, M.; Le Scouarnec, R.; Lecommandoux, S.; Harrisson, S.; Bonduelle, C., Memory Effect in Thermoresponsive Proline-based Polymers. *Angew. Chem. Int. Ed.* **2022,** *61* (46), e202209530.
51. Yan, D.; Müller, A. H. E.; Matyjaszewski, K., Molecular Parameters of Hyperbranched Polymers Made by Self-Condensing Vinyl Polymerization. 2. Degree of Branching. *Macromolecules* **1997,** *30* (23), 7024-7033.
52. Wolf, F. K.; Frey, H., Inimer-Promoted Synthesis of Branched and Hyperbranched Polylactide Copolymers. *Macromolecules* **2009,** *42* (24), 9443-9456.
53. Vlasov, G. P.; Tarasenko, I. I.; Pankova, G. A.; Il'ina, I. E.; Vorob'ev, V. I., Hyperbranched polylysines: Mechanism of formation. *Polym. Sci., Ser. B* **2009,** *51* (7-8), 296-302.
54. Min, K.; Gao, H., New Method To Access Hyperbranched Polymers with Uniform Structure via One-Pot Polymerization of Inimer in Microemulsion. *J. Am. Chem. Soc.* **2012,** *134* (38), 15680-15683.
55. Li, P.; Dong, C.-M., Phototriggered Ring-Opening Polymerization of a Photocaged l-Lysine N-Carboxyanhydride to Synthesize Hyperbranched and Linear Polypeptides. *ACS Macro Lett.* **2017,** *6* (3), 292-297.
56. Aydogan, C.; Ciftci, M.; Yagci, Y., Hyperbranched Polymers by Light-Induced Self-Condensing Vinyl Polymerization. *Macromol. Rapid Commun.* **2018,** *39* (15), e1800276.
57. Li, P.; Song, Y.; Dong, C.-M., Hyperbranched polypeptides synthesized from phototriggered ROP of a photocaged Nε-[1-(2-nitrophenyl)ethoxycarbonyl]-l-lysine-N-carboxyanhydride: microstructures

and effects of irradiation intensity and nitrogen flow rate. *Polym. Chem.* **2018,** *9* (29), 3974-3986.
58. Yang, N.; Jiang, Y.; Tan, Q.; Ma, J.; Zhan, D.; Wang, Z.; Wang, X.; Zhang, D.; Hadjichristidis, N., One-Pot Structure-Controlled Synthesis of Hyperbranched Polymers by a "Latent" Inimer Strategy Based on Diels–Alder Chemistry. *Angew. Chem. Int. Ed.* **2022,** *61*, e202211713.
59. Ge, Y.; Li, P.; Guan, Y.; Dong, C.-M., Hyperbranched polylysine: Synthesis, mechanism and preparation for NIR-absorbing gold nanoparticles. *Chin. Chem. Lett.* **2019,** *30* (7), 1428-1431.
60. Li, F.; Cao, M.; Feng, Y.; Liang, R.; Fu, X.; Zhong, M., Site-Specifically Initiated Controlled/Living Branching Radical Polymerization: A Synthetic Route toward Hierarchically Branched Architectures. *J. Am. Chem. Soc.* **2018,** *141* (2), 794-799.
61. Tao, W.; Liu, Y.; Jiang, B.; Yu, S.; Huang, W.; Zhou, Y.; Yan, D., A Linear-Hyperbranched Supramolecular Amphiphile and Its Self-Assembly into Vesicles with Great Ductility. *J. Am. Chem. Soc.* **2011,** *134* (2), 762-764.
62. Liu, Y.; Yu, C.; Jin, H.; Jiang, B.; Zhu, X.; Zhou, Y.; Lu, Z.; Yan, D., A Supramolecular Janus Hyperbranched Polymer and Its Photoresponsive Self-Assembly of Vesicles with Narrow Size Distribution. *J. Am. Chem. Soc.* **2013,** *135* (12), 4765-4770.
63. Jiang, W.; Zhou, Y.; Yan, D., Hyperbranched polymer vesicles: from self-assembly, characterization, mechanisms, and properties to applications. *Chem. Soc. Rev.* **2015,** *44* (12), 3874-3889.
64. Liu, S.; Gao, Y.; Zhou, D.; Zeng, M.; Alshehri, F.; Newland, B.; Lyu, J.; O'Keeffe-Ahern, J.; Greiser, U.; Guo, T.; Zhang, F.; Wang, W., Highly branched poly(β-amino ester) delivery of minicircle DNA for transfection of neurodegenerative disease related cells. *Nat. Commun.* **2019,** *10* (1), 3307.
65. Zeng, M.; Xu, Q.; Zhou, D.; A, S.; Alshehri, F.; Lara-Sáez, I.; Zheng, Y.; Li, M.; Wang, W., Highly branched poly(β-amino ester)s for gene delivery in hereditary skin diseases. *Adv. Drug Delivery Rev.* **2021,** *176*, 113842.
66. Tshepelevitsh, S.; Kütt, A.; Lõkov, M.; Kaljurand, I.; Saame, J.; Heering, A.; Plieger, P. G.; Vianello, R.; Leito, I., On the Basicity of Organic Bases in Different Media. *Eur. J. Org. Chem.* **2019,** *2019* (40), 6735-6748.
67. Zheng, Y.; Li, S.; Weng, Z.; Gao, C., Hyperbranched polymers: advances from synthesis to applications. *Chem. Soc. Rev.* **2015,** *44* (12), 4091-4130.
68. Nwajiobi, O.; Verma, A. K.; Raj, M., Rapid Arene Triazene Chemistry for Macrocyclization. *J. Am. Chem. Soc.* **2022,** *144* (10), 4633-4641.

For Table of Contents Only